

Near-Surface Wind, SLP and SST: Some Inter-relationships and a Set of Corrections for Wind Trends 1949-1988

M. Neil Ward

Hadley center for Climate Prediction and Research
London Road, Bracknell, Berkshire RG12 2SY

Introduction

Cardone et al. (1990) (hereafter, CGC, 1990) and others suggest that the wind speed reported by ships has increased in recent decades due to changes in observational practices. The main cause that they identify is an increasing fraction of anemometer readings, typically now made at a mean height of 20 m, relative to Beaufort force estimates, which are converted to 10 m winds (using a biased conversion scale) before insertion into computerized datasets like COADS.

This paper aims to contribute to the debate on the reliability of the wind data, and on how to maximize its utility for climate studies. The first section below describes the data and basic processing methods, followed by a discussion of some theoretical relationships that are expected to exist between near-surface wind and sea-level pressure (SLP), and a description of the balanced friction flow (BFF) method for deriving nearsurface seasonal mean wind from seasonal mean SLP patterns. To gain confidence in the observed wind and SLP data, it is useful to verify the presence of relationships in the data that are expected from theory. The process is two-way, since the data are also verifying the theory. The next two sections consider a dataset of calculated BFF winds for 1949-88, and present a comparison with the reported observed winds; the trends in the observed wind time-series are adjusted to equal the trends in the BFF time-series, thereby calculating a corrected wind dataset. A wind correction method based on this approach assumes that there is no substantial time varying bias in the estimated pressure gradients, and that the distance between derived wind trend and observed wind trend can be used to isolate time varying bias in wind observation. The derived wind is a function of pressure difference, so will largely be independent of any time-varying bias that may exist in ship pressure data, though other problems such as changes in bias towards reports during fair weather may influence the derived wind trends in some regions. The corrections reported here follow on from those reported in Ward (1992). Finally, two applications of the corrected wind data are reported. Firstly, we illustrate the impact of the corrections on estimated wind patterns associated with multi-decadal rainfall fluctuations in sub-Saharan Africa. Secondly, very close agreement is found in the year-to-year variability of nearsurface divergence patterns (calculated from the corrected wind) and sea-surface temperature (SST) patterns in the tropical western Pacific. The close agreement illustrates the excellent value of the ship data for climate studies once it has been processed carefully.

Data and Basic Processing

Near-surface marine atmosphere

The Comprehensive Ocean-Atmosphere Data Set (COADS) 2° lat \times 2° long (2×2) trimmed monthly means for the years 1949-88 were used for the analyses (Woodruff et al., 1987). Seasonal mean anomaly datasets were constructed on the 10° lat \times 10° long grid-scale for the variables SLP, zonal wind component (u) and meridional wind component (v). Details of the data processing are in Ward (1992, 1994). The basic procedure was:

- Construct smoothed $2^\circ \times 2^\circ$ climatologies.
- Construct $2^\circ \times 2^\circ$ seasonal mean anomaly datasets.
- Construct $10^\circ \times 10^\circ$ anomalies by averaging all constituent $2^\circ \times 2^\circ$ anomalies, weighting for the number of observations that contributed to each $2^\circ \times 2^\circ$ anomaly. At least 20 observations were required to form a $10^\circ \times 10^\circ$ anomaly.

Sea-surface temperature

SST data were taken from the Meteorological Office Historical Sea-surface Temperature dataset version 4 (MOHSST4) (Bottomley et al., 1990). The data were formed into 10° lat \times 10° long seasonal anomalies (details in Ward, 1992, 1994).

Deriving Wind from Sea-Level Pressure

The seasonal mean horizontal momentum equation can be simplified by assuming a three-way balance of forces between seasonal mean SLP (P), seasonal mean friction and seasonal mean coriolis force (f). To a first approximation, it has often been assumed that friction direction opposes the motion, and that the force is directly proportional to wind speed through a constant (k) called the coefficient of surface resistance. Then the horizontal momentum equation can be solved for u and v :

$$u = \frac{kP_x + fP_y}{k^2 + f^2} \quad v = \frac{kP_y - fP_x}{k^2 + f^2} \quad (1)$$

where

$$P_x = -\frac{1}{\rho} \frac{\partial P}{\partial x} \quad P_y = -\frac{1}{\rho} \frac{\partial P}{\partial y}$$

Such a derived wind is often described as “balanced friction flow” (BFF). In deriving Eq. (1), all terms are time and area averages, and all eddy terms are ignored (validity discussed in Ward, 1994). To apply Eq. (1), assumptions have to be made about the value of k . Typical values of k have been estimated in the range $1-3 \times 10^{-5} \text{s}^{-1}$ (e.g. Gordon and Taylor, 1975). Note that as well as varying geographically due to varying mean boundary layer characteristics, k will also depend on location within the boundary layer. For example, Brummer et al. (1974) reports an experiment in the North Atlantic trades at 10°N in which they found that the friction

force declined by a factor of two between 15 m and 500 m, such that the implied value of k falls from about $2.3 \times 10^{-5} \text{ s}^{-1}$ to $1.2 \times 10^{-5} \text{ s}^{-1}$.

It follows from Eq. (1) that k and f prescribe the backing angle (β_F) and ratio (R_F) of the BFF vector to the geostrophic vector:

$$\tan \beta_F = \frac{k}{f} \quad (2a)$$

$$R_F = \sqrt{\left(\frac{f^2}{f^2 + k^2} \right)} \quad (2b)$$

For the studies in this paper, values of k are derived by assuming a backing angle β_F of 10° for the regions polewards of 50° , and 50° for the average of regions equatorwards of 10° . Backing angles are linearly interpolated over the latitude range 10° - 50° , assuming 50° at 10° latitude and 10° at 50° latitude. The values of k that these backing angles imply are broadly consistent with the results of previous studies (e.g. Gordon and Taylor, 1975).

Comparison of Observed and Derived Winds 1949-88

The BFF equations (Eq. 1) have been applied to every seasonal mean SLP anomaly field 1949-88. (Note that the BFF equations can be solved using anomalies, whereas the inclusion of the advective accelerations would require the use of the total wind since advection of anomalies is being effected by actual winds, not just the anomalies). Where possible, missing SLP anomalies were spatially interpolated using a simple linear system (Ward, 1994).

Figure 1 illustrates time-series of derived BFF and observed wind anomalies for a 10×10 box in the tropical North Atlantic (Fig. 1a) and a box in the tropical South Atlantic (Fig. 1b). The impression is gained that interannual variability of the observed and derived winds agree very well. Figures 2a-d show the correlation of derived and observed wind anomalies over 1949-88 for the seasons Dec-Feb (DJF) and Jul-Sep (JAS). There are many regions where the correlation is >0.7 , giving good confidence in the reliability of the data and the BFF theory. The poor performance in some equatorial regions is probably because so close to the equator the equations can be less applicable, and SLP needs to be resolved on a finer spatial scale. The improvement over the geostrophic approximation (see Fig. 2e) is, not surprisingly, most apparent in the tropics, where the improvement in the simulation of the v wind component is significantly greater than that of the u wind component.

In Fig. 1, it is also clear that despite good interannual agreement, there is a systematic difference in the trends of the BFF and observed wind. In both instances, the observed wind shows a trend towards strengthening easterlies, whereas in the BFF wind, the trends are much reduced or absent.

To give a clear picture of global changes in reported and derived wind circulation strength, global mean zonal wind anomaly time-series of the observed, provisionally corrected (from Ward, 1992) and new BFF wind have been calculated as follows (series were calculated for each of the four seasons separately):

(i) Reject all those 10×10 boxes with

$$\frac{|\bar{u}|}{\sigma_u} < 1.282 \quad (3)$$

where \bar{u} is the particular season's $10^\circ \times 10^\circ$ climatological zonal wind (calculated using the period 1969-88) and σ_u is the standard deviation of the zonal seasonal values over 1969-88. Following normal distribution theory, this criterion ensures that series included in the analysis have less than 10% of seasonal values with a wind vector of sign opposite to the mean vector. Those series with a negative mean zonal wind were multiplied by -1 so that the series effectively represent anomalies in the *magnitude* of the zonal wind. While it is tempting to simply analyze trends in the modulus of the zonal wind, this should not be done, because such a quantity is also a function of data reliability, which of course shows a trend through time.

(ii) Standardize each 10×10 series over the period 1949-1988.

(iii) Average the standardized anomalies over all ocean regions.

The mean standardized anomaly time-series for each of the four seasons are plotted together in Fig. 3. The reported wind time-series shows a mean increase of about one standard deviation. The provisionally corrected and new derived wind time-series show no significant trend.

Revised Corrections for Ship Reports of Near-Surface Wind 1949-88

In this section, the correction methodology outlined in Ward (1992) is applied, but using the new BFF derived winds in place of the geostrophic wind used in Ward (1992). Also, the analysis here is on the 10×10 scale, compared to 2×2 in Ward (1992), so data coverage is much better, affording a more complete coverage for the corrections.

The analysis includes only u and v seasonal wind time-series which have a long-term u or v mean that is substantially different from zero (based on Eq. 3; details in Ward, 1994). So trends in these series can be used to approximate trends in the strength of the circulation. The difference in trend over 1949-88 (termed a_1 , units are $\text{ms}^{-1}\text{yr}^{-1}$) between the BFF wind and observed wind is estimated (for u and v separately). Then the linear component of the implied spurious percentage increase S in the observed wind vector over 40 years is

$$S = \left(\frac{a_1 x 40}{\bar{V}_a} \right) * 100 \quad (4)$$

where \bar{V}_a the climatological wind in either zonal or meridional direction, depending on whether the u or v wind is being analyzed. For a given box, up to 8 estimates of S were available (u and v in the 4 seasons). The estimates were averaged, weighting each S as in Ward (1992) by its estimated "reliability", calculated as the 1949-88 derived versus observed wind

correlation (r , examples in Fig. 2a-d) multiplied by the number of years with data (N). To smooth the field of $10^\circ \times 10^\circ$ values, a zonally directed weighting scheme of 2:4:2, with one unit of weight each to the boxes to the north and south, was superimposed on the “reliability” weight calculated for each box ($N*r$). If a box did not have a value of S , it was given the area average (before application of the smoothing), using the areas defined in Ward (1992). For equatorial boxes (10°N - 10°S), one further smoothing was applied by averaging the target box, the box to the north and the box to the south, weighting according to the sum of the weights that had contributed to each of the boxes in the first smoothing pass. The final result is shown in Fig. 4.

The weighted average of all values of S before smoothing is 14.3%, which is very similar to the overall average of 16.1% calculated in Ward (1992). Ives (1987) shows maps of the percentage of wind reports that contained the code for an anemometer reading in the British Met. Office Marine Data Bank in differing periods, the last of which is 1975-1979. Her maps generally support the geographical variations of S in Fig. 4. Regions that still have low ratios of measured to estimated winds (such as North Atlantic) are expected to have the smallest corrections. However, the *negative* corrections in the far North Atlantic (also found in Ward, 1992) remain unexplained.

Corrected wind datasets have been calculated using the method in Ward (1992). For each 10×10 vector wind time series, the corrected data are calculated:

$$\tilde{u} = u_t - [u_t * (S/100) * (t - t_b) / 40] \quad (5)$$

$$\tilde{v} = v_t - [v_t * (S/100) * (t - t_b) / 40]$$

where \tilde{u}_t and \tilde{v}_t , are the corrected u and v seasonal wind vectors for time t , u_t and v_t , are the observed COADS seasonal wind vectors for t , and S is the 1949-88 mean spurious percentage change in wind speed for the 10×10 box. Note that the mid-point of the season is used for t (e.g. July-September 1949, $t=1949.71$). t_b is an arbitrarily selected time which acts as the base time for the corrections. For example, if $t_b=1949.0$, then when $t=1949.0$, $\tilde{u} = u$ and $\tilde{v} = v$; 40 years later when $t=1989.0$, the wind vectors are reduced in magnitude by $S\%$, (or increased by $S\%$ if S is negative). To correct the data for use in the studies reported here, t_b was always set to the mid-point of the 1969-1988 normals period.

Applications of the Corrected Wind Data

Circulation associated with extended Sahel drought

It is known that JAS rainfall in the Sahel region of sub-Saharan Africa was dramatically less in the period 1969-88 than in the period 1949-68. Figure 5 shows the composite difference 1969-88 minus 1949-68 for (a) the raw observed near-surface wind data and (b) the corrected data. Compared to the raw data, the corrected data suggest some quite different aspects to the tropical circulation changes:

(i) In the tropical Atlantic, the raw data emphasize enhancement of easterly trades near 15°N during the drought period, whereas the corrected data suggest modest enhancement, linking with circulation changes in the equatorial and South Atlantic that correspond to a

weakening of cross equatorial flow. The corrected wind pattern suggests a much stronger modulation of the local Hadley circulation, and the corrected wind pattern is likely to have significant consequences for ocean circulation and cross-equatorial heat fluxes in the western equatorial Atlantic.

(ii) In the northern Indian Ocean, the raw data suggest a strengthening of the monsoon circulation in the Sahel drought period, whereas the corrected data indicate little change or a slight weakening in the monsoon circulation, which is more consistent with the slight reduction in Indian monsoon rainfall 1969-88.

(iii) In the tropical Pacific, the raw data suggest strengthened circulation in many regions, whereas the corrected data suggest little change in circulation strength, but some changes in the meridional wind.

The corrections make little difference to the circulation change in the extra tropical North Atlantic, which is dominated by an anomalous anticyclonic circulation centered near the UK during the Sahel drought period.

The relationship between near-surface divergence and SST in the western Pacific.

In the tropics, direct forcing of the near-surface atmosphere by SST will lead to a close association between anomalies of near-surface convergence and SST maxima in the absence of other forcing (Lindzen and Nigam, 1987).

This section studies the relationship between SST and near-surface divergence in the tropical western Pacific. A $10^\circ \times 10^\circ$ dataset of near-surface divergence was calculated using finite differences of the $10^\circ \times 10^\circ$ seasonal mean vector wind anomalies. Where possible, missing SLP anomalies were spatially interpolated using a simple linear system (Ward, 1994). To further reduce noise, the divergence anomalies were zonally smoothed, weighting 1:2: 1.

The first JAS SST EOF for 1949-88 (Fig. 6a) in the tropical western Pacific is an east-west dipole pattern. In the west, the largest weights are at 0° - 10° S. (The pattern for 1904-90 is very similar (Fig. 6b), supporting the stability of the result). The first JAS divergence EOF (Fig. 6c) has a more complicated pattern. Over the equatorial latitudes 10° N- 10° S it is also an east-west dipole. Again, largest weights in the west are at 0° - 10° S. In the west, the pattern is also a north-south dipole, with large positive weights centered at 0° - 10° S and large negative weights at 10° - 20° N. (Also, in the east, the weights at 10° - 20° N and at 10° - 20° S have a sign that is opposite to the weights at 10° S- 10° N.)

The correlation between the time-coefficients of SST EOF1 and divergence EOF1 is extremely high (Fig. 6d). So we suggest that, in the region of the EOF analysis, the equatorial atmosphere is responding directly to the SST as predicted by Lindzen and Nigam (1987), especially at 0° - 10° S in the western Pacific. At 10° - 20° N, the atmosphere does not appear to be responding so directly to the local SST. One hypothesis is that equatorial regions of enhanced near-surface convergence lead to a zone of diabatic heating anomaly (enhanced penetrative convection leading to enhanced latent heating), which leads to descent and near-surface divergence anomalies about 10° latitude polewards, which is consistent with the meridional overturning found by Gill (1980) in response to a line of heating in the tropical atmosphere.

That an SST and near-surface divergence time-series can be derived with such near-perfect agreement (Fig. 6d) is extremely encouraging for the utility of ship data in climate studies. As illustrated here, the data can be used to test and explore theories on the relationship between SST and atmospheric circulation.

Discussion and Conclusions

Based on comparisons with the derived BFF wind, this paper estimates that the globally averaged spurious percentage rise in reported wind speed over 1949-88 is 14.3%. This is very similar to the estimate of 16.1% made in Ward (1992). Applying the theory of CGC (1990), such estimates suggest an increase from 0% of anemometer readings in 1949 to 60% of anemometer readings in 1988. However, there is considerable uncertainty as to the fraction of ship wind reports that are based on anemometers around the world (Kent and Taylor, 1991; Ive, 1987).

The results of Ive (1987) suggest more anemometer readings than WMO (1990), but considerably less than the 60% needed for the theory of CGC (1990) to explain the mean value of S calculated above. Thus there may be further cause of the spurious rise in wind speeds. For example, it is possible that there has been a gradual change in the way observers translate sea states into Beaufort numbers. This possibility is suggested by the results of Lindau et al. (1990) who performed a SLP-wind comparison for the $10^\circ \times 10^\circ$ box centered 15°S , 35°W in the tropical South Atlantic. They analyzed only those reports that were stated to be estimated, but still found a spurious rise in the reported wind speed. One possibility is that as anemometers have become widely available, so reporters have tended to tune their estimated winds to that which anemometers typically give. Indeed, it is likely that some reports coded as estimated have in fact been influenced by the presence of an anemometer on board.

The corrections reported in this paper vary sufficiently smoothly and are sufficiently complete to enable the regional correction approach in Ward (1992) to be replaced by a field of smooth corrections (Fig 4). So the new corrected wind data do not have sharp discontinuities across regional boundaries and are therefore potentially well suited to estimations of horizontal divergence, or to forcing ocean numerical models. The new corrections are also much more reliable in the tropics because the BFF method used to derive the wind is one that is well suited to the tropical boundary layer on the seasonal time-scale. Indeed, recent analyses (e.g. Neelin, 1989, Philander, 1990) have pointed out the similarity of the BFF equations with equations used elsewhere to understand the tropical atmosphere. The BFF system is similar to the equations used by Gill (1980) to boundary layer to heating from the SST. Finally, the BFF system is also similar to the atmospheric part of many simple coupled tropical ocean-atmosphere models.

Some analysis of the terms excluded in the BFF equations is given in Ward (1994). For example, on the $10^\circ \times 10^\circ$ spatial scale, acceleration was found to be important only in a small number of boxes, notably the cross equatorial Indian monsoon flow in boreal summer. The potential importance of the transient eddy friction term, the spatial eddy friction term and the spatial eddy coriolis term were all illustrated. Nonetheless, maps have been presented in this paper (Fig. 2) showing generally good correlation (resulting from the non-trend time scale) between winds derived using BFF and the uncorrected observed wind, suggesting good reliability in both data and theory. Once the spurious wind trend is removed, it is suggested that the ship reported SLP and the corrected wind data form an extremely valuable climate research tool. Two examples of applications to climate studies have been given. Firstly, compared to the raw data, the corrected data give a substantially different picture of tropic-wide circulation changes associated with sub-Saharan drought over recent decades. Secondly, the corrected data were used to create a near-surface divergence dataset. Divergence is a notoriously difficult quantity to estimate, but the near-perfect agreement between the time-series of the first SST

EOF and first near-surface divergence EOF in the tropical western Pacific over 1949-88 suggests that the data processing employed here has enabled the calculation of a useful divergence dataset.

References

- Brummer, B., Augstein, E., and Richl, H., 1974: On the low-level wind structure in the Atlantic trade. *Quart. J. Roy. Meteor. Soc.*, 100, 109-121.
- Bottomley, M., Folland, C.K., Hsiung, J., Newell R.E., and Parker D.E., 1990: Global ocean surface temperature atlas (GOSTA). Joint Meteorological Office/Massachusetts Institute of Technology Project. Project supported by US Dept. of Energy, US National Science Foundation and US Office of Naval Research Publication funded by UK Depts. of Energy and Environment. pp20 and 313 Plates. HMSO, London.
- Cardone, VJ., Greenwood, J.G., and Cane, M.A., 1990: On trends in historical marine wind data, *J. Climate*, 3, 113-127.
- Gill, A E., 1980: Some simple solutions for heat-induced tropical circulation. *Quart. J. Roy. Meteor. Soc.*, 106,447-462.
- Gordon, A H., and Taylor, RC, 1975: Computations of surface layer air parcel trajectories, and weather, in the oceanic tropics. International Indian Ocean Expedition, Meteorological Monographs, No. 7, Univ. Press of Hawaii Honolulu, 112 pp.
- Isemer, H.-J., and Hasse, L, 1991: The scientific Beaufort equivalent scale: Effects on wind statistics and climatological air sea flux estimates in the North Atlantic Ocean. *J. Climate*, 4, 819-836.
- Ive, D.S., 1987: A comparison of numbers of visually estimated and instrumentally measured wind data. Marine Tech Note No. 2, pp43. Available from the National Meteorological Library, Meteorological Office, Bracknell, Berkshire, UK.
- Kent, EC., and Taylor, P.K, 1991: Ships observing marine climate - A catalogue of the voluntary observing ships participating in the VSOP-NA. Marine meteorology and related oceanographic activities, Report No. 25, WMO/TD-No. 456. pp 123.
- Lindau, R., Isemer, H J., and Hasse, L, 1990: Towards time dependent calibration of historical wind observations at sea. *Trop. Ocean-Atmos. Newsletter*, Spring 1990, 712.
- Lindzen, RS., and Nigam, S., 1987: On the role of sea surface temperature gradients in forcing low-level winds and convergence in the tropics. *J. Atmos. Sci.*, 44, 2418-2436.
- Neelin, J.D., 1989: On the interpretation of the Gill Model. *J. Atmos. Sci.*, 46, 2466-2468
- Philander, S.G., 1990: *El Niño, La Niña, and the Southern Oscillation*. International Geophysics Series, Vol. 46, Academic Press, San Diego, London, 293 pp.
- Ward, M.N., 1992: Provisionally corrected surface wind data, worldwide ocean-atmosphere surface fields and Sahelian rainfall variability. *J. Climate*, 5, 454-475.
- Ward, M.N., 1994: Tropical North African rainfall and worldwide monthly to multidecadal climate variations. Ph.D. thesis, Reading University, pp 313.
- WMO, 1990: International list of selected, supplementary, and auxiliary ships, (1990 edition -magnetic tape version) WMO-47, World Meteorological Organization, Geneva.
- Woodruff, S.D., Slutz, RJ., Jenne, R L, and Steurer, P.M., 1987: A comprehensive Ocean-Atmosphere data set. *Bull. Amer. Meteor. Soc.*, 68, 1239-1250.

Figure 1: Raw observed (solid) and derived Balanced Friction Flow (dashed) seasonal zonal wind anomaly time-series. The smooth lines are fitted using a filter with 50% amplitude cut-off at about 6 years. The centre of the $10^\circ \times 10^\circ$ box is indicated alongside the panel. Anomalies for each season are plotted.

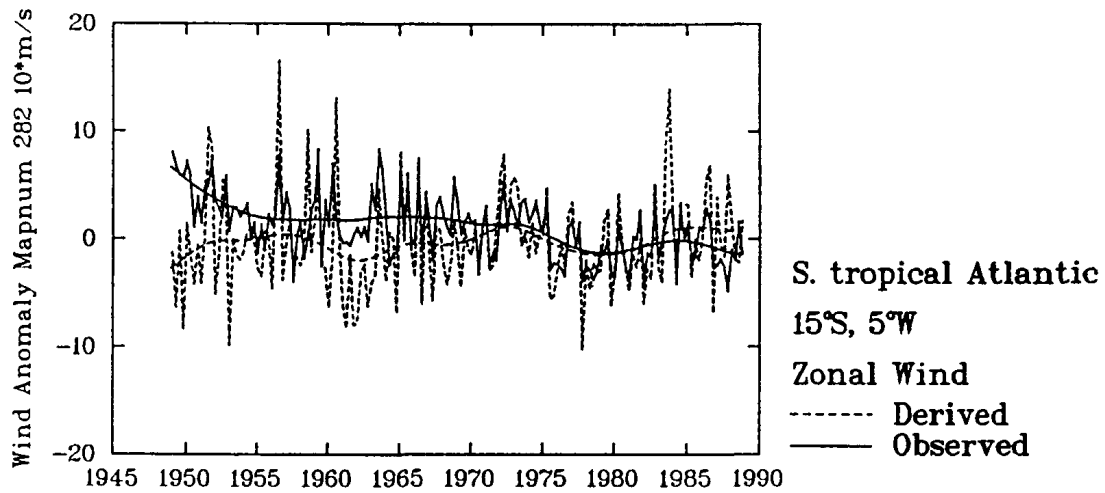
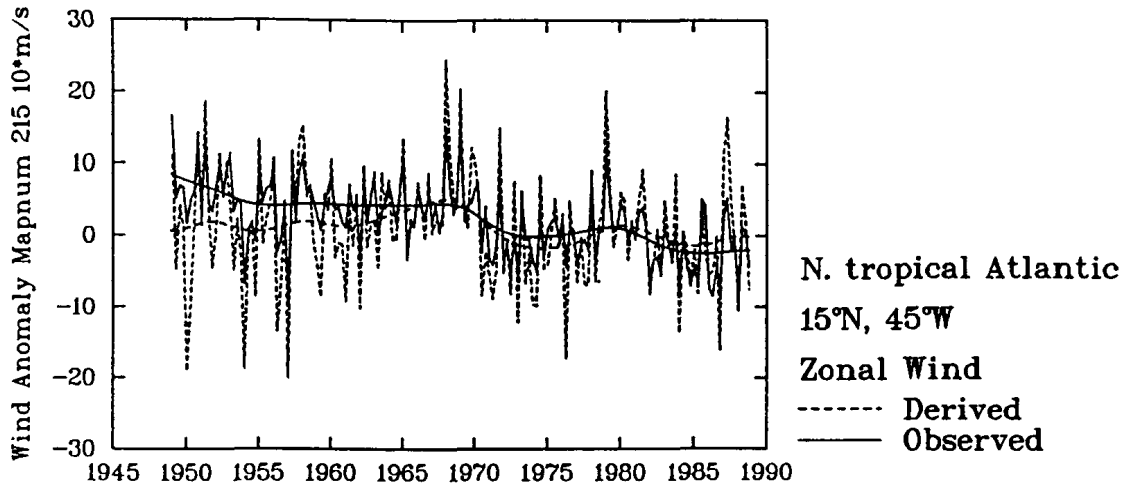


Figure 2a: Correlation ($\times 100$) over 1949-88 between time-series of observed wind and time-series of derived balanced friction flow (BFF) wind. Values >0.7 are shaded with dots, values <0.3 are cross-hatched. (a) u-wind in DJF. (b) v-wind in DJF. (c) u-wind in JAS. (d) v-wind in JAS.

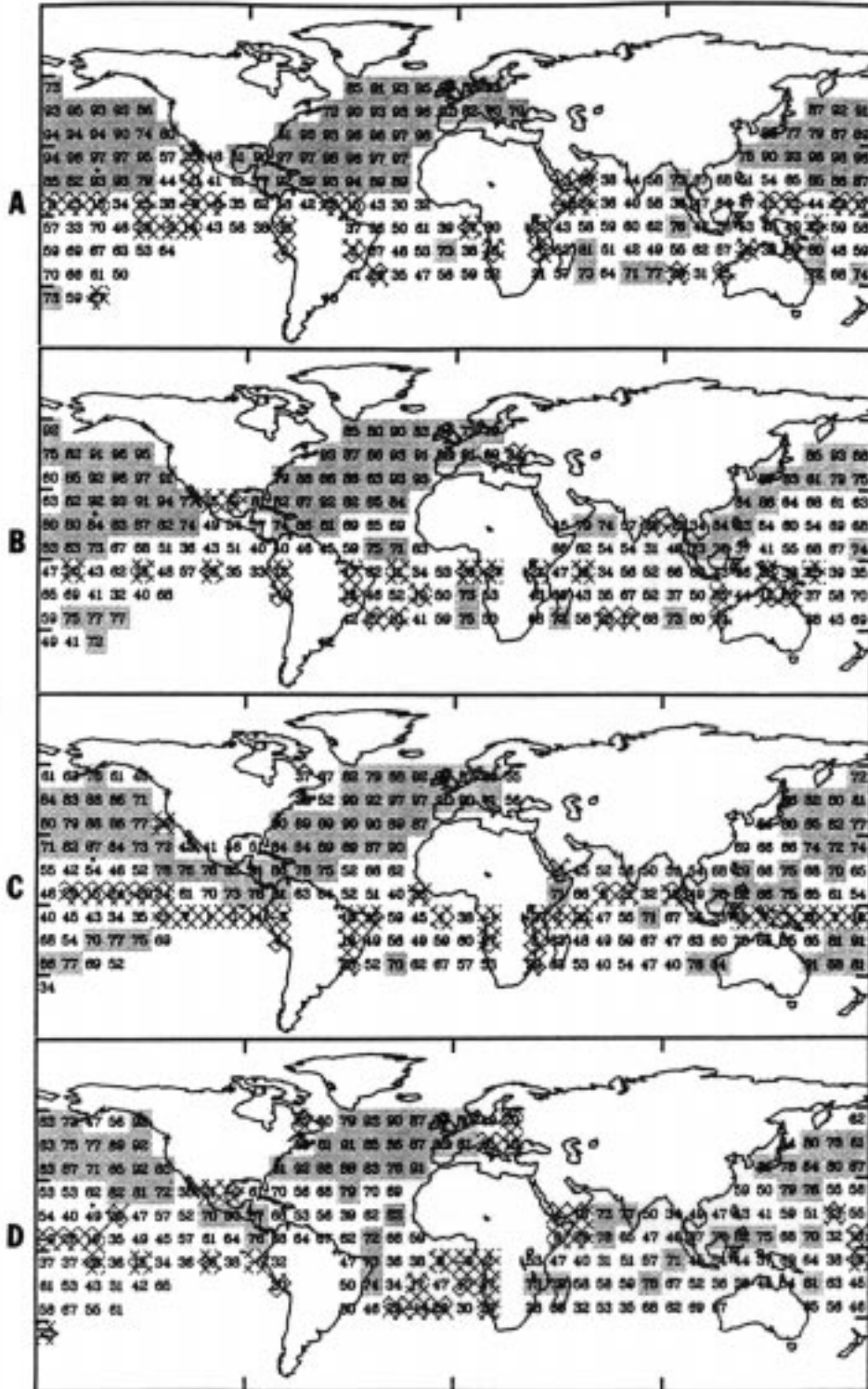


Figure 2b: Mean correlation as a function of latitude for BFF wind versus observed wind (solid) and geostrophic wind versus observed wind (dashed). Bottom panels show the number of correlations that were available for averaging at each latitude.

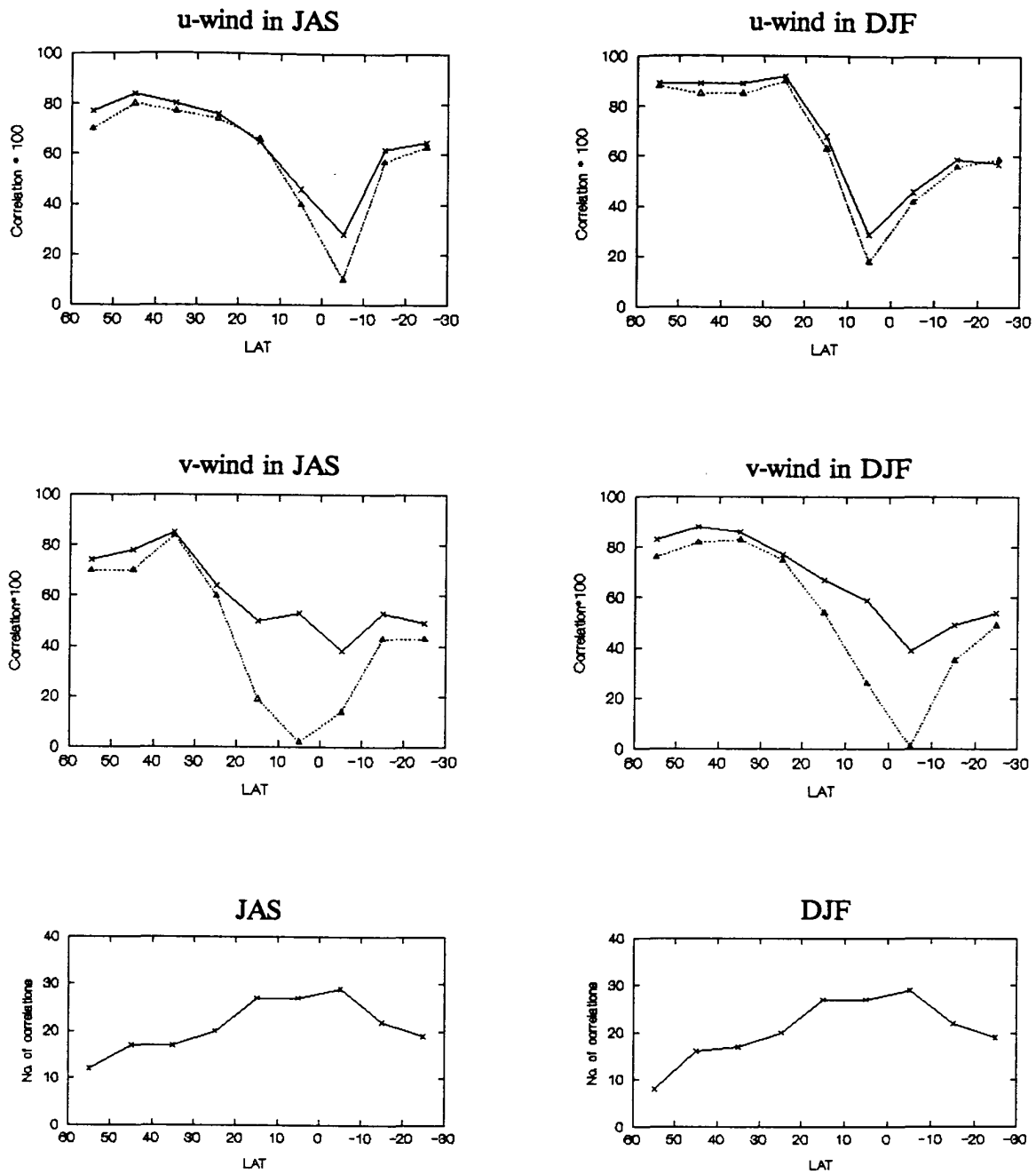


Figure 3: Mean standardised anomaly of zonal wind in each season 1949-88, for (i) reported wind, (ii) provisional corrected wind (version 1, based on Ward, 1992) and (iii) balanced friction flow wind. The value plotted for each season is the average of the standardized anomalies in all available $10^\circ \times 10^\circ$ ocean boxes. The series shown effectively indicates the magnitude of the zonal wind vector, since all the contributing $10^\circ \times 10^\circ$ series with a negative mean were multiplied by -1 prior to analysis, and all time-series with a mean close to zero were rejected (see text for more details).

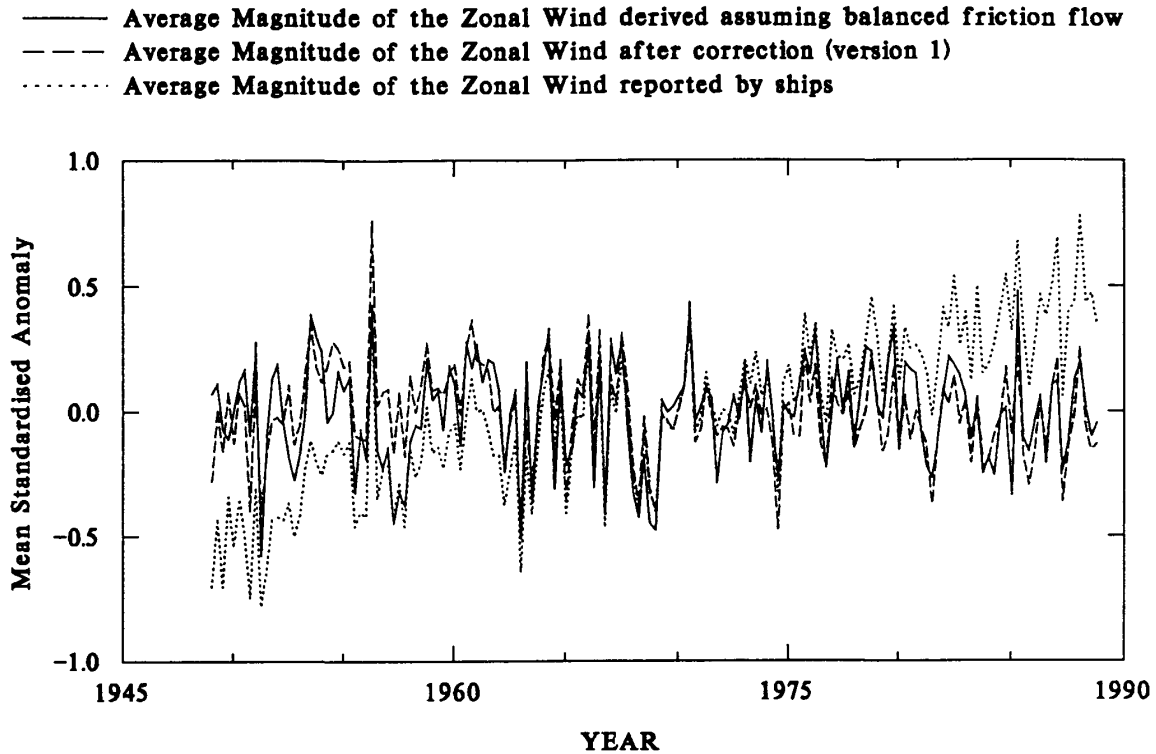


Figure 4: The difference between the increase in the magnitude of the observed wind and the increase in the magnitude of the balanced friction flow wind over 1949-1988, expressed as a percentage of the magnitude of the mean observed wind (the values are referred to as S in the text). Values shown were derived by averaging estimates of S based on u-wind and v-wind series for each of the four seasons. The values were then spatially smoothed.

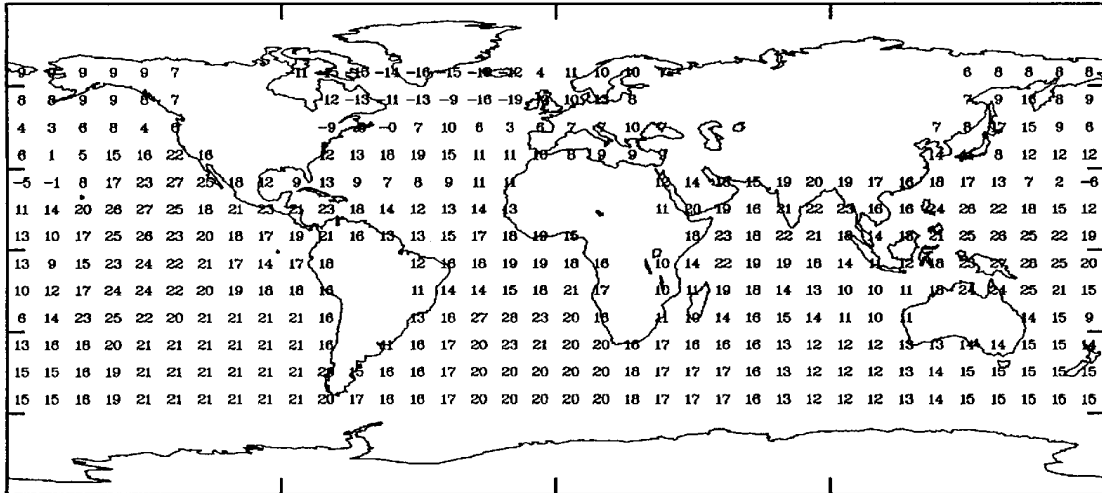


Figure 5a: Composite difference (1969-88 MINUS 1949-68) for July-September of the near-surface Raw wind.

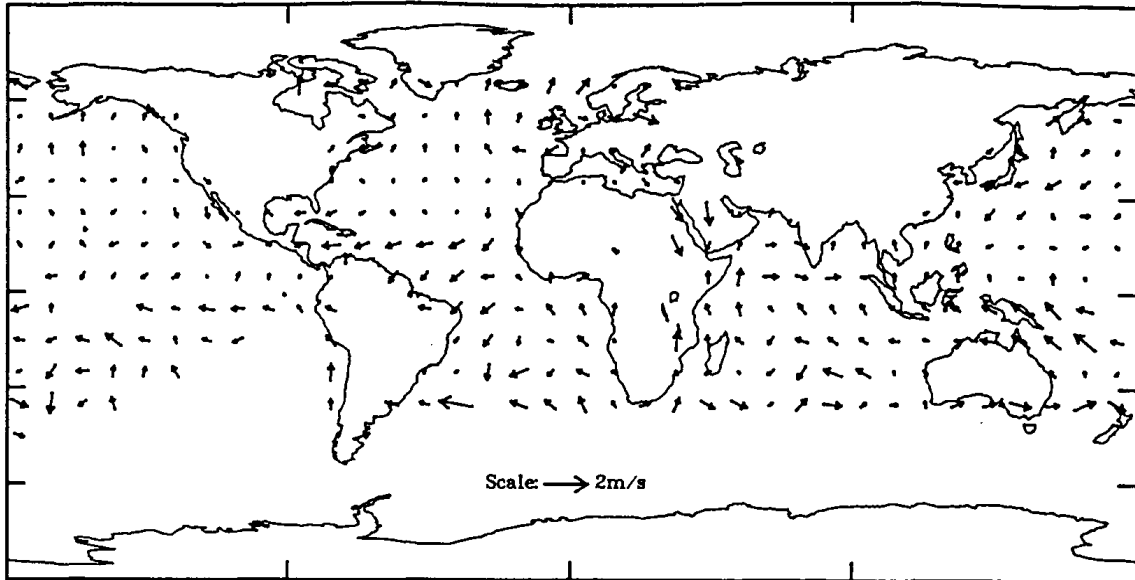


Figure 5b: Composite difference (1969-88 MINUS 1949-68) for July-September of the Corrected wind.

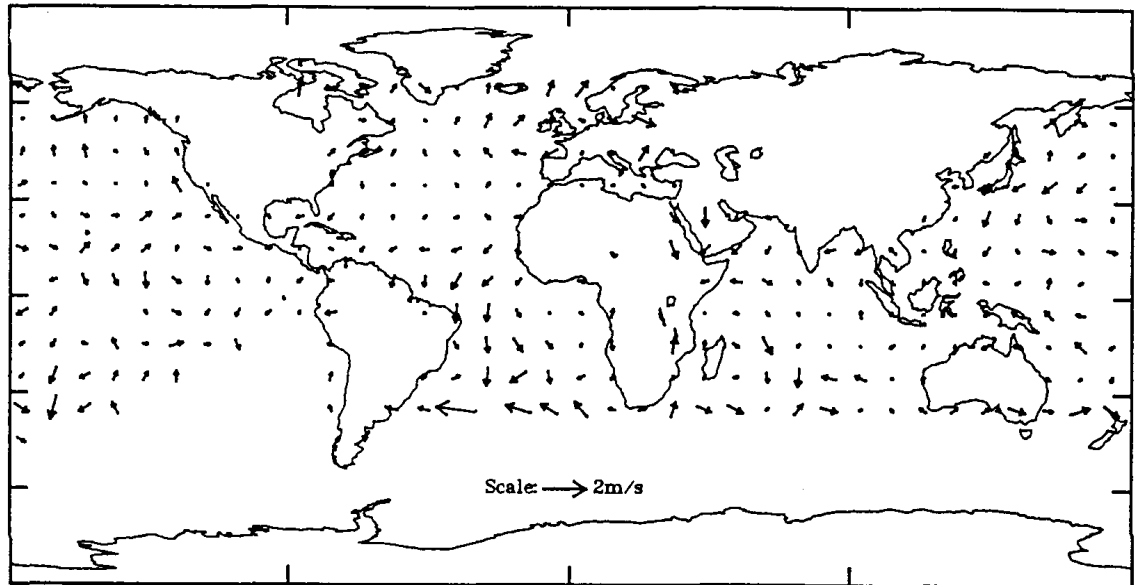


Figure 6a: First correlation EOF 1949-88 for $10^\circ \text{ lat} \times 10^\circ \text{ long}$ JAS SST anomalies in the tropical central and western Pacific (28.6% of total variance).

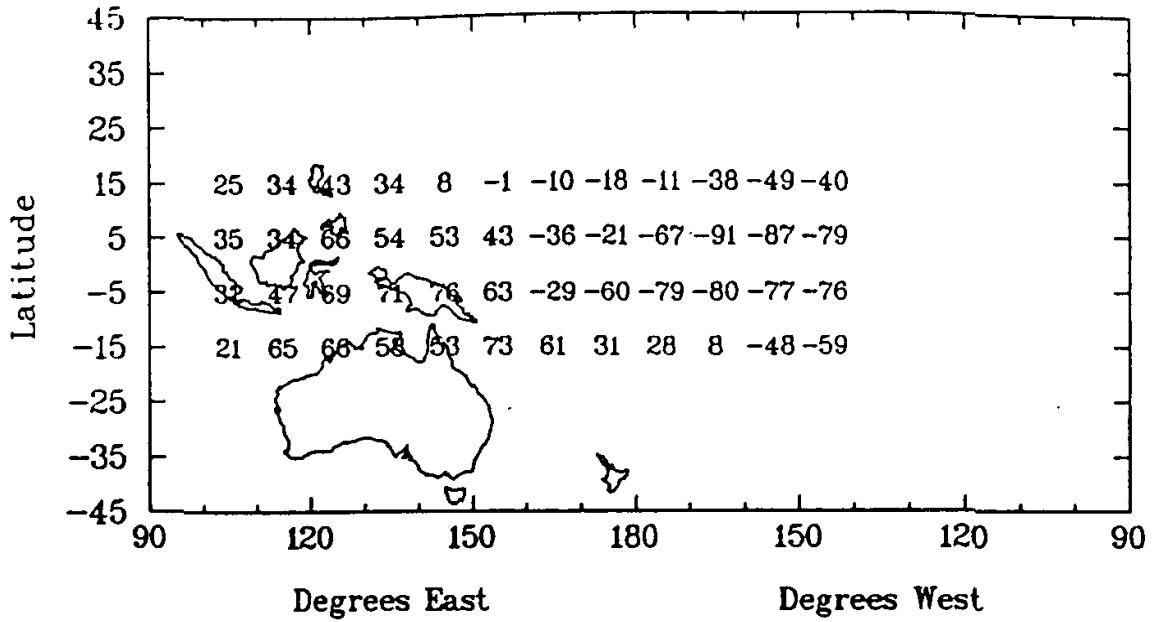


Figure 6b: Same as (a) but for 1904-90 (21.6% of total variance).

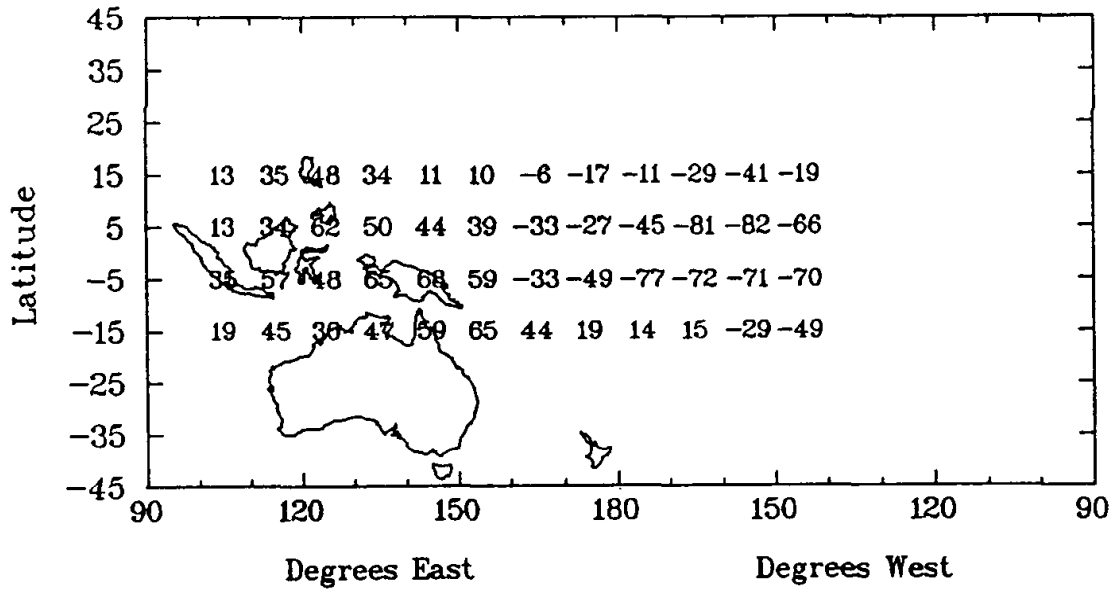


Figure 6c: Same as (a) but for near-surface divergence 1949-88 (35.2% of total variance). All series were high-pass filtered prior to analysis (passing timescales <11.25 years).

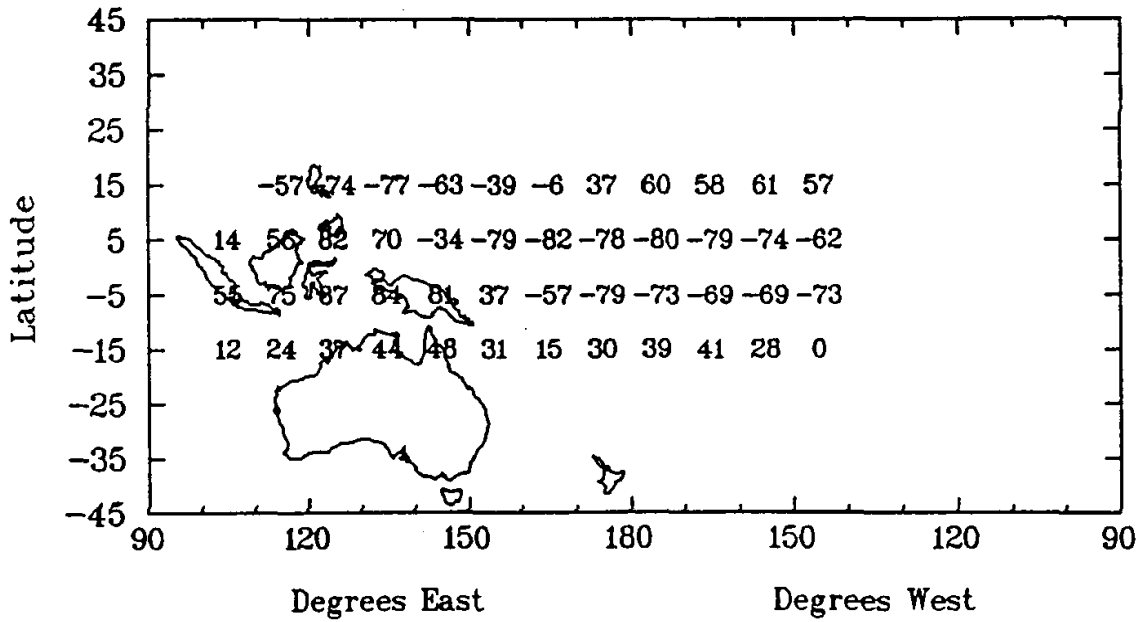


Figure 6d: Observed JAS time coefficients 1949-88 of tropical central and western Pacific SST EOF1 in Fig. 6a (solid line with crosses) and near-surface divergence EOF1 in Fig. 6c (dashed line).

